Supplementary Material

Tuning the Photocatalytic Activity of Ti-based LDH via Divalent Cations for Enhanced Tetracycline Hydrochloride Degradation

Xiangtai Zhang[1], Tao Feng[1,2]*, Si Wu[1,2]*, Tingpeng Chen[1], Yuqi Tang[1], Yu Shi[3]

[1] College of Resources and Environmental Engineering, Wuhan University of Science and Technology, Wuhan, 430081, China

[2] Hubei Key Laboratory for Efficient Utilization and Agglomeration of Metallurgic Mineral Resources. Wuhan University of Science and Technology, Wuhan, 430081, China

[3] Wuhan Jincheng Yida Technology Development Co., Ltd. Wuhan, 430081, China

*Corresponding Authors

E-mail: fengtaowhu@163.com (T. Feng)

E-mail: siwu@wust.edu.cn (S. Wu)

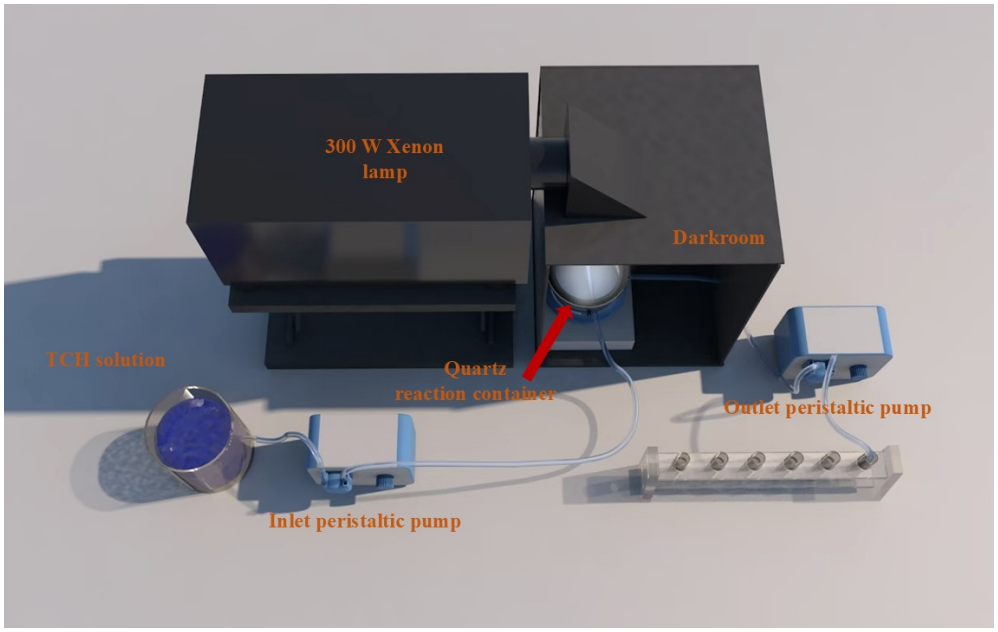

Fig. S1 Diagram of the dynamic adsorption photocatalytic device.

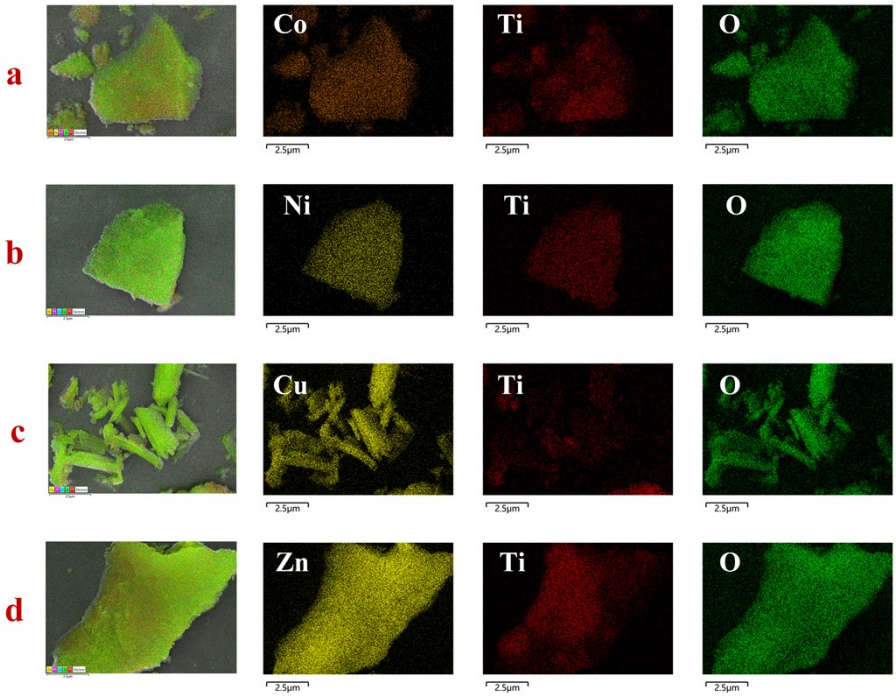

Fig. S2 EDS element distribution diagrams of different MTi-LDHs (a: CoTi-LDH; b: NiTi-LDH; c: CuTi-LDH; d: ZnTi-LDH).

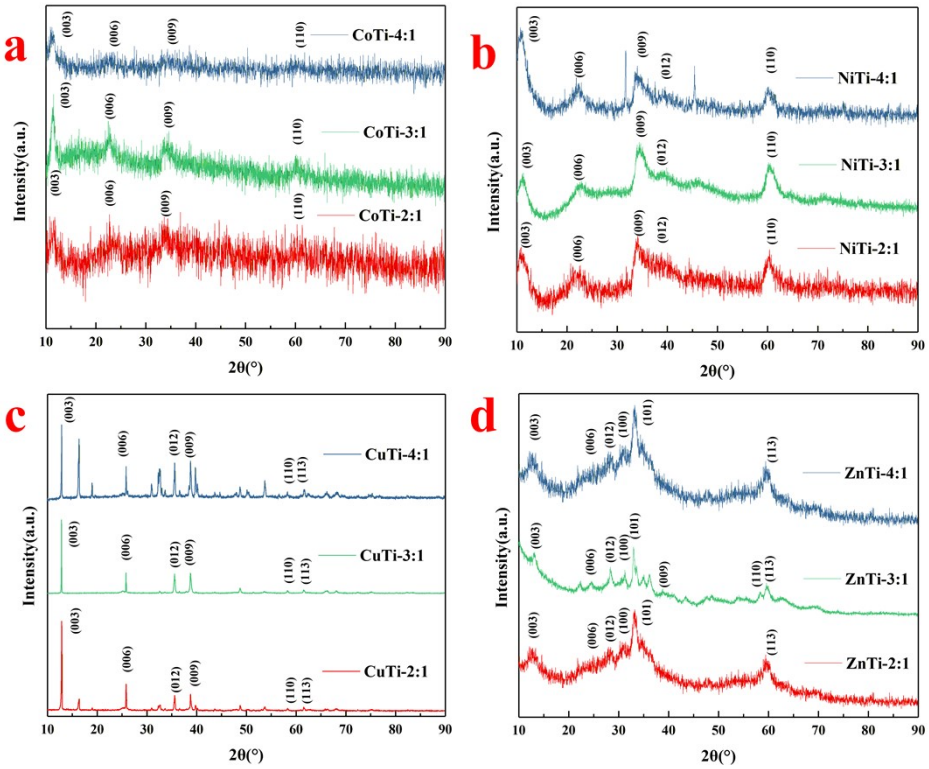

Fig. S3 XRD patterns of MTi-LDHs with different M^{2+}:Ti (a: CoTi-LDH; b: NiTi-LDH; c: CuTi-LDH; d: ZnTi-LDH).

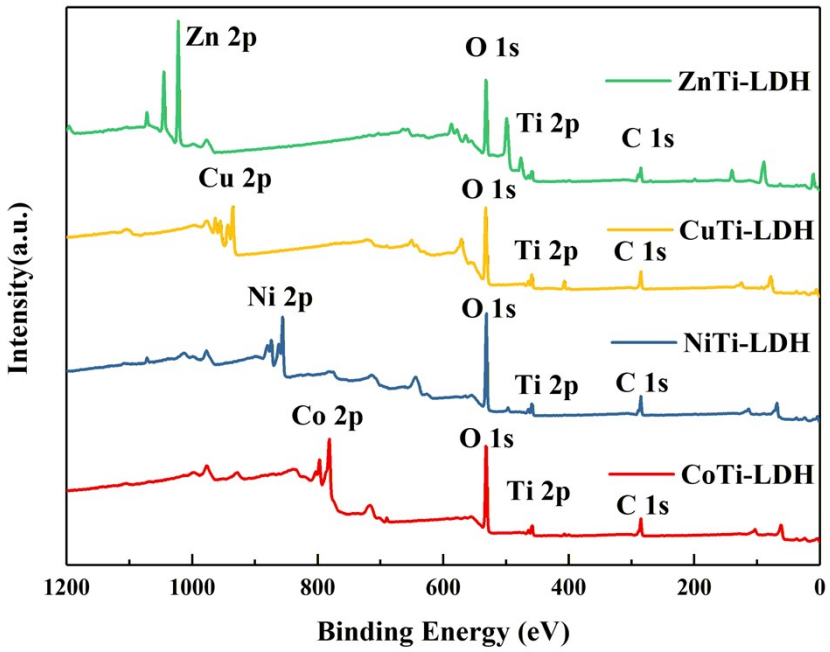

Fig. S4 XPS survey of MTi-LDHs.

Table S1 The XPS Peak positions of each element in MTi-LDHs.

MTi-LDH	C 1s(eV)		O 1s(eV)		Ti 2p(eV)		M 2p (M=Co,Ni,Cu,Zn)(eV)	
	C 1s	C 1s	O 1s	O 1s	Ti 2p 1/2	Ti 2p 3/2	M 2p 1/2	M 2p 3/2
CoTi-LDH	288.72	284.80	531.31	529.61	463.85	458.10	796.63	780.82
NiTi-LDH	288.81	284.80	530.92	529.56	463.95	458.15	873.05	855.59
CuTi-LDH	288.36	284.80	531.07	529.59	464.01	458.29	954.57	934.86
ZnTi-LDH	288.22	284.80	531.4	529.59	463.82	458.16	1044.89	1022.73

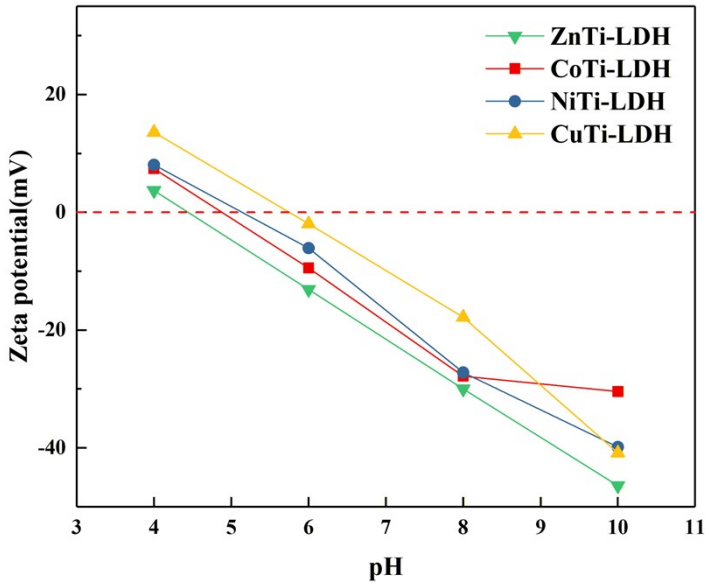

Fig. S5 Zeta potential curve for different MTi-LDHs.

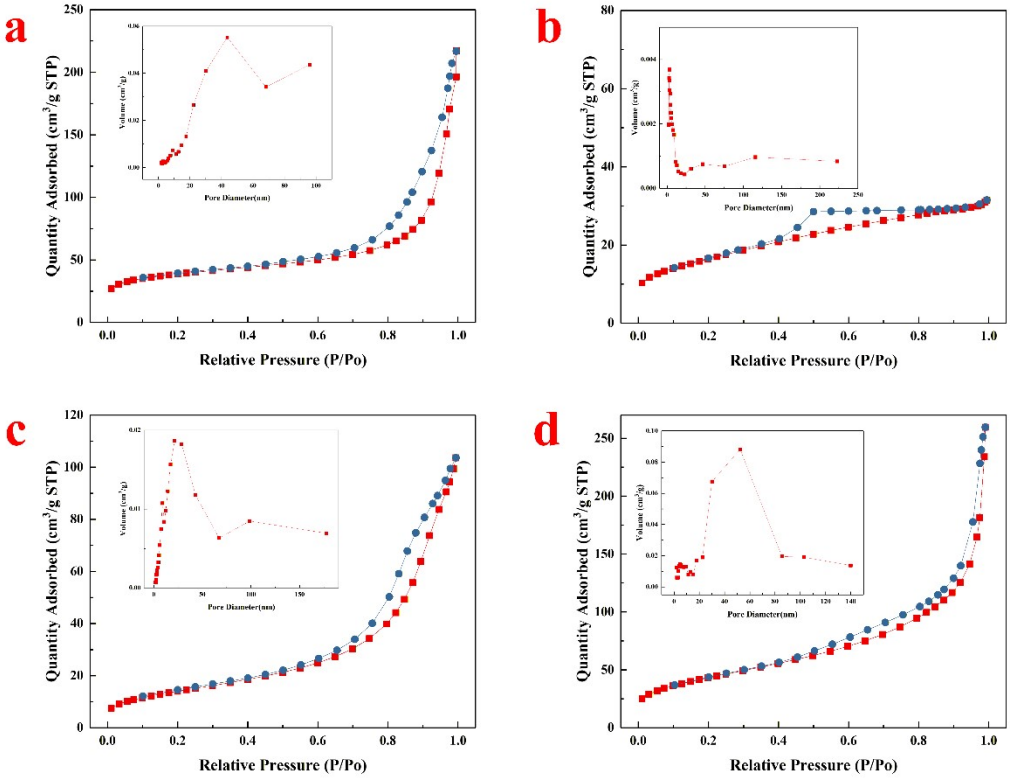

Fig. S6 Nitrogen adsorption-desorption isotherms and corresponding pore size distribution curves of MTi-LDHs (a: CoTi-LDH; b: NiTi-LDH; c: CuTi-LDH; d: ZnTi-LDH).

Table S2 Textural parameters obtained from BET of MTi-LDHs.

Sample	BET Surface Area (m^2/g)	BJH volume of pores (cm^3/g)	Average pore diameter (nm)
CoTi-LDH	139.2	0.28	9.3
NiTI-LDH	58.9	0.05	3.3
CuTi-LDH	51.8	0.16	12.4
ZnTi-LDH	156.8	0.41	10.2

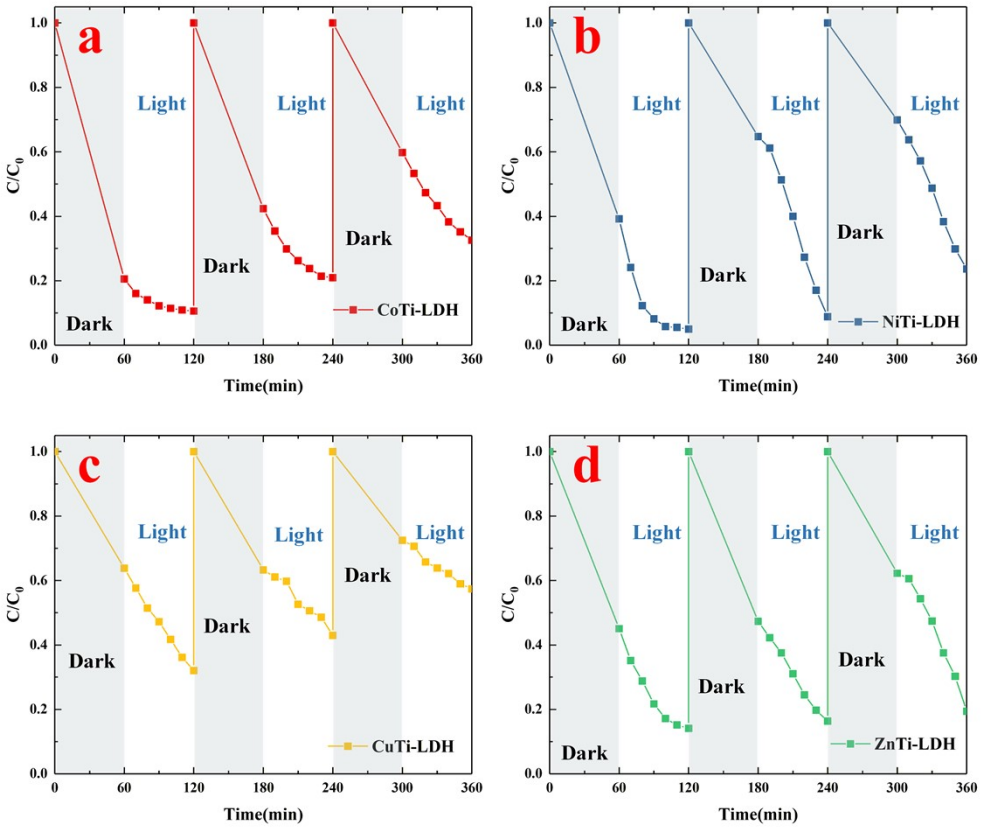

Fig. S7 Recycling Performance of MTi-LDH in the photocatalytic degradation of TCH (a: CoTi-LDH; b: NiTi-LDH; c: CuTi-LDH; d: ZnTi-LDH).

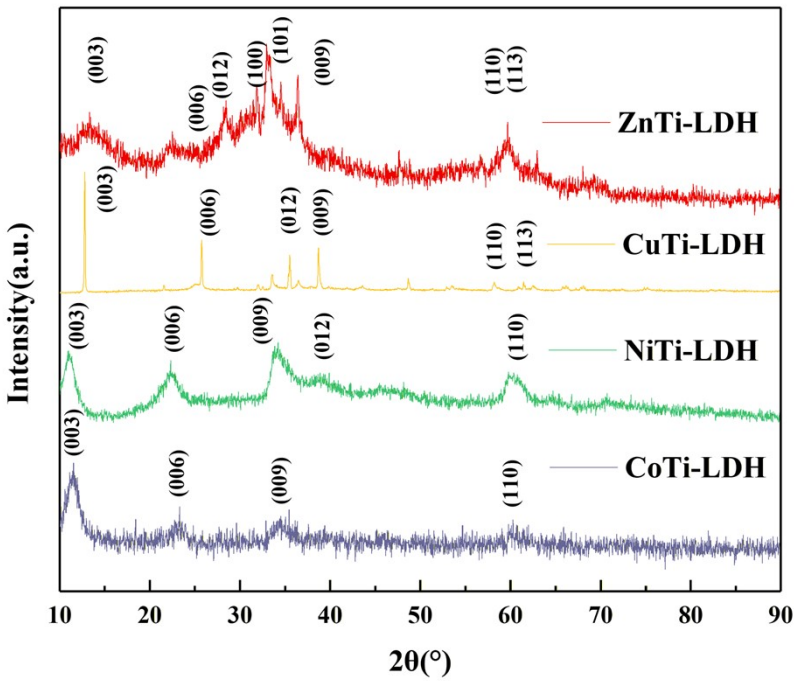

Fig. S8 The XRD patterns of the MTi-LDH samples after TCH degradation.

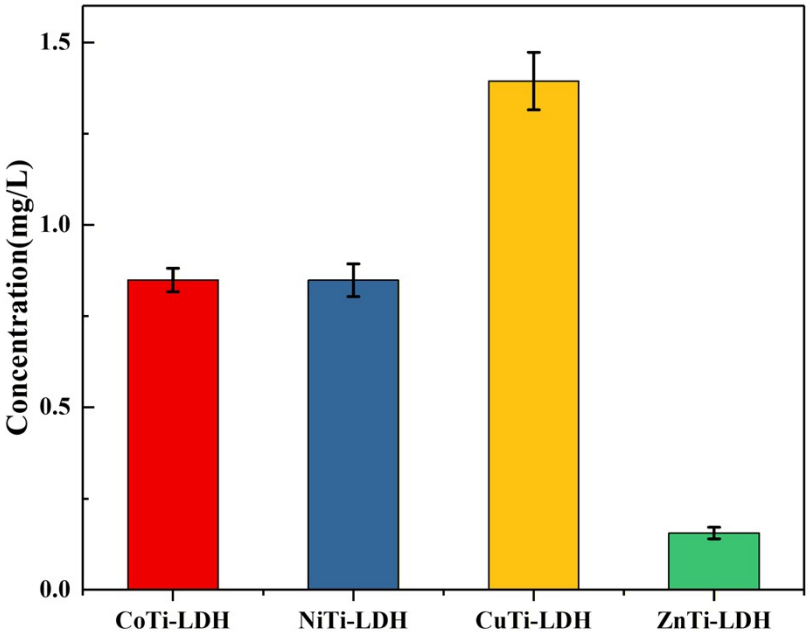

Fig. S9 Metal Leaching concentrations for MTi-LDHs catalysts after 150 min leaching.

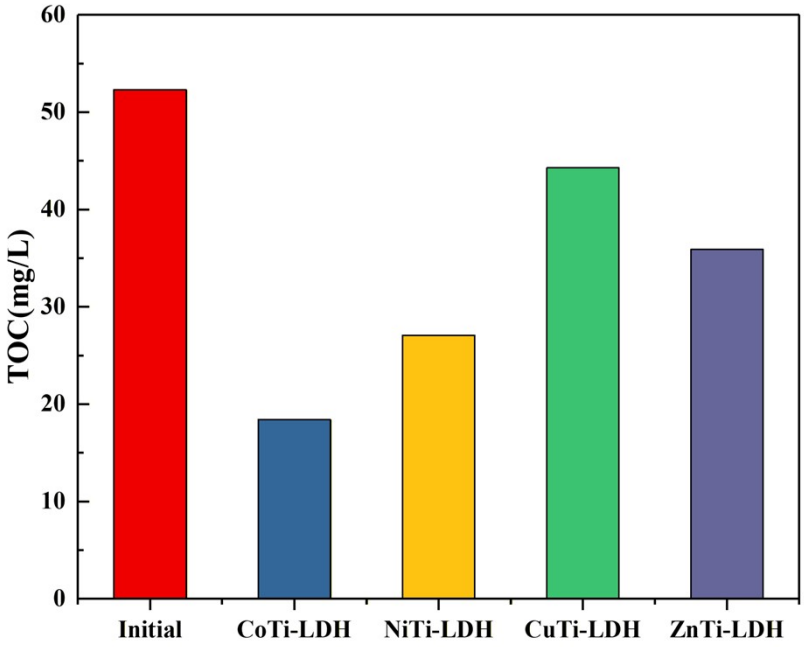

Fig. S10 The TOC concentration of TCH samples treated by MTi-LDHs.

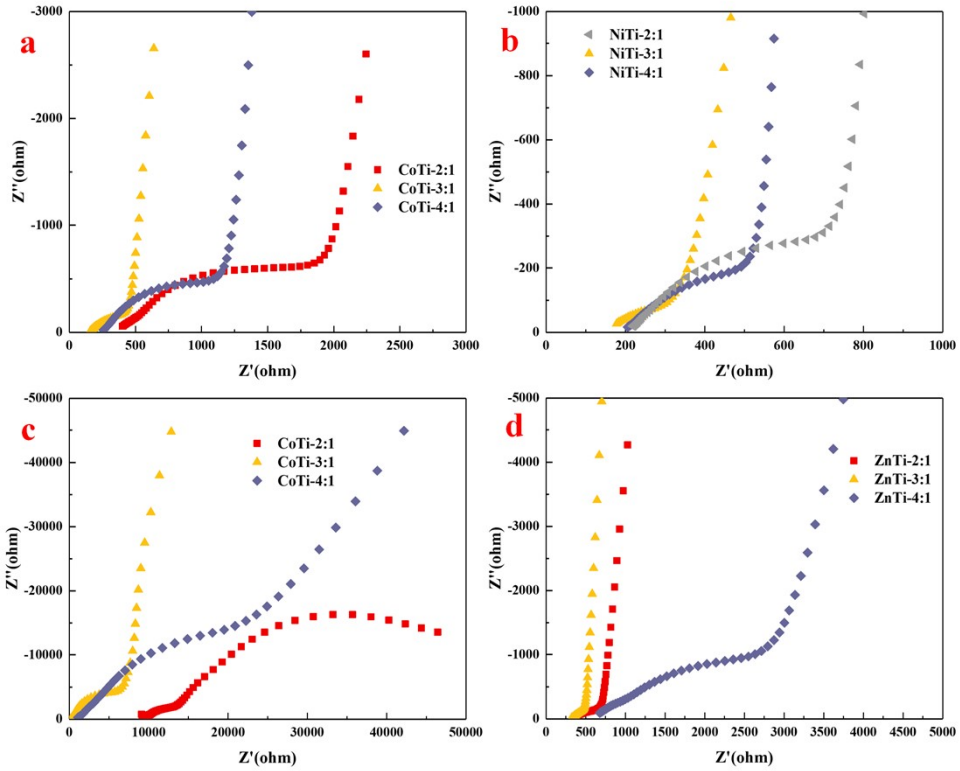

Fig. S11 Nyquist plots of electrochemical impedance spectra (EIS) of MTi-LDHs with different M^{2+}:Ti (a: CoTi-LDH; b: NiTi-LDH; c: CuTi-LDH; d: ZnTi-LDH).

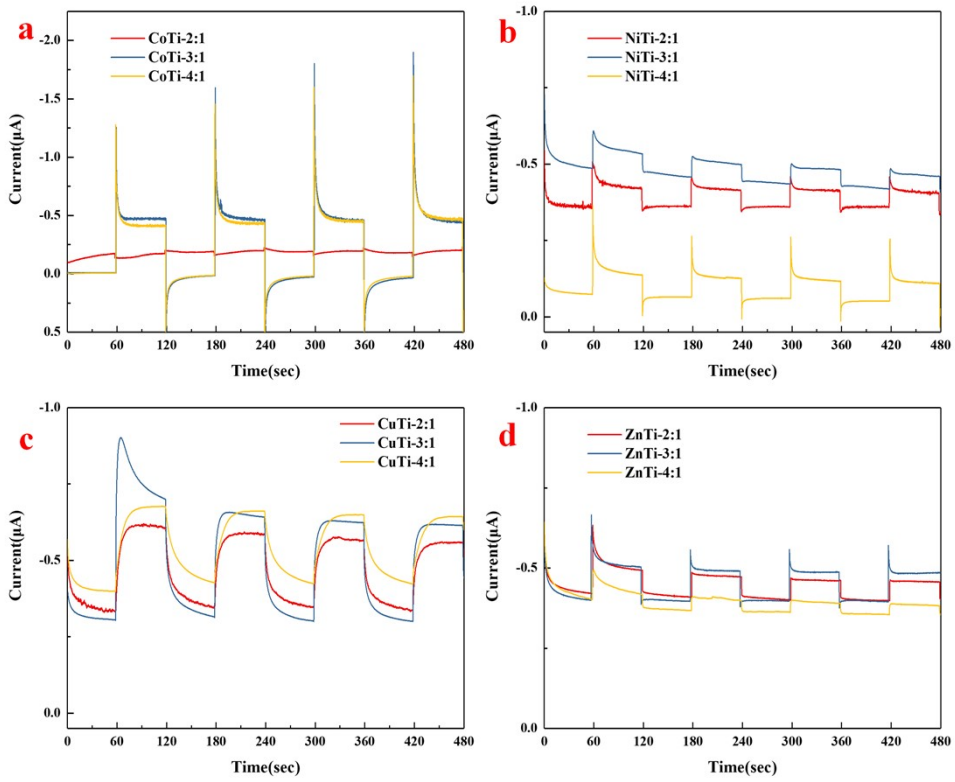

Fig. S12 Transient photocurrent curves (i-t) for MTi-LDHs with different M^{2+}:Ti (a: CoTi-LDH; b: NiTi-LDH; c: CuTi-LDH; d: ZnTi-LDH).

Tables S3 Effect of different scavengers (IPA, BQ, AO, L-His) on the degradation process of MTi-LDHs.

Condition	Apparent rate constants (k,min^{-1})			
	CoTi-LDH	NiTi-LDH	CuTi-LDH	ZnTi-LDH
Non	0.0189	0.0191	0.0151	0.0247
IPA	0.0185	0.0184	0.0144	0.0245
BQ	0.0088	0.0121	0.011	0.0113
AO	0.0176	0.0132	0.013	0.0244
L-His	0.0082	0.0093	0.0028	0.0194

Table S4 The contribution of various pathways on TCH degradation process of MTi-LDHs.

Active species	CoTi-LDH	NiTi-LDH	CuTi-LDH	ZnTi-LDH
·OH	0.021	0.037	0.046	0.008
$\cdot O_2^-$	0.534	0.366	0.272	0.542
h^+	0.068	0.309	0.139	0.012
$^1O_2$	0.566	0.513	0.814	0.214